Improved Segmentation for Intravascular Ultrasound (IVUS) Modality

Suhaili Beeran Kutty[1,3]*, Rahmita Wirza O.K Rahmat[1], Sazzli Shahlan Kassim[2], Hizmawati Madzin[1], Hazlina Hamdan[1]

¹Faculty of Computer Science and Information Technology, Universiti Putra Malaysia, Serdang, Malaysia
²Faculty of Medicine, Universiti Teknologi MARA, Sungai Buloh, Malaysia
³Faculty of Electrical Engineering, Universiti Teknologi MARA, Shah Alam, Malaysia
*Corresponding author E-mail:suhaili88@salam.uitm.edu.my

Abstract

IVUS is the modality to investigate the internal structure of the coronary artery. Segmentation is necessary to differentiate the lumen, the media-adventitia and others feature that appears on the modality, but manual segmentation is tedious and time-consuming. To enhance the computational segmentation, this paper presents the process to segment catheter shape, inner and outer layer of the artery. The new algorithm is proposed to detect the catheter shape and percentage of the accuracy is 100%. We also provide information on detection of lumen and media-adventitia border and area using a parametric deformable model algorithm with gradient vector flow as the external force. The Percentage Area of Difference (PAD) value for the segmentation is below than one, indicate that this proposed method is highly encouraging for IVUS segmentation process. Based on the inner border detected, media-adventitia boundaries also can be detected without manual initialization points. This work is important to facilitate the process of the 3D reconstruction of the coronary artery.

Keywords: Catheter Detection; Coronary Artery; Intravascular Ultrasound; IVUS Segmentation; Parametric Deformable Model.

1. Introduction

IVUS segmentation refers to the process to detect and identify certain structures within the IVUS image[1]. The structures including the catheter shape, area and border of the lumen, area, and border of media-adventitia and the plaque distribution. The purpose of the detection is to allow the measurement of the artery in term of shape, area, thickness and eccentricity [2], [3]. In other words, IVUS segmentation helps in measuring the cross-sectional area of the vessel [4]. From the measurement, it helps to quantify the plaque burden that exists between the lumen and media-adventitia borders [5], [6]. Furthermore, the plaque distribution according to the types and volume could be characterized [7].

The importance of the computational IVUS segmentation was supported by the drawbacks of the manual routine. [2]–[4] agreed that manual segmentation is tedious and time-consuming. Inter- and intra-observer variability also one of the factors why computational IVUS segmentation is urgently needed [3], [5]. Inter-observer variability is referring to the variation of the finding or result when two or more observers diagnose the same subject, whereas the intra-observer is the variation of finding from one observer when she/he diagnoses the same subject for multiple times. Besides that, the expert also needs to deal with a series of images either in the same modality or not [8].

IVUS segmentation is necessary because it will subdivide the image into separate regions for further investigation and process [9]. The shortcoming of previous IVUS segmentation process has ignored the appearance of the catheter shape [4]. However, this shape is important because it is one of correspondence mark when the cardiologist refers to the Angiography modality. Another drawback in IVUS segmentation approach is to transform the original image to the polar format and needs several steps of image enhancement before the segmentation process takes place. This practice can degrade the quality of the image. Furthermore, to improve the ability of IVUS segmentation, the techniques should allow media-adventitia area detection automatically. Thus, the objective of this paper is to propose a novel IVUS segmentation approach in addressing those issues. We have proposed to detect catheter shape region that appears on the IVUS image using threshold normalization and extracts the boundary using labeling technique. Then, the parametric deformable model is used to detect an area of the lumen. Finally, we manage to detect the media-adventitia based on the lumen boundary results.

The next section of this paper is literature review where we discuss the existing research on IVUS segmentation. After that, we cover the methodology of this work starting with image preprocessing to the outer layer detection. We present our finding in the result and discussion section. Lastly is our conclusion toward this IVUS segmentation process.

2. Literature Review

The process of IVUS segmentation consists of image acquisition, pre-processing and filtering, border and structures detection and some works came out with plaque classification such as [10]. There are a lot of studies on IVUS segmentation [7], [11]–[18], where the early studies had been reviewed by Katauzian *et al.* in [9].

Recently, Su *et al.* in [5] proposed to combine Artificial Neural Network (ANN) and active contour model to segment lumen and media-adventitia layer. In [19], they used Fuzzy approach combined with Haar wavelet to detect the lumen. Debarghya China *et*

al. [20] suggested initialization points between lumen and media-adventitia layer and used random walks algorithm to segment the inner layer. Yan and Cui [3] used fuzzy connectedness algorithm and image gradient where they highlight three features of IVUS image. The features are lumen area consists of homogeneous intensity; media-adventitia border has high gradient value and lumen border also has high gradient value but less than media-adventitia border. Based on these features, the IVUS image needs to be transformed into the polar image before it can be segmented. Media-adventitia border detection based on Otsu thresholding approach had been proposed by Sofian *et al.* [1]. They used the detected threshold value for morphological operations, erosion, and dilation. Hamdi *et al.* [10] used contourlet transform approach to filter the IVUS images before the morphological snake algorithm is used to segment lumen and media adventitia. The concept of the algorithm is a morphological discretization of the Partial Differential Equations (PDE) of curve evolution of the geodesic active contours in a level set framework.

Temporal texture and analysis is the method used by Chen & Gangidi to determine lumen and media-adventitia border or external elastic membrane (EEM) [21]. The concept they applied in their segmentation is lumen contour can be traced based on finest texture and homogeneous intensity. After that, the media-adventitia border can be detected based on the coarse-most texture located outside the lumen border. They used IVUS images in polar format.

Sun *et al.* [22] presented IVUS segmentation method using graph-based approach. The system allowed refinement from user to correct the segmentation. In [23], Lazrag & Naceur proposed IVUS segmentation method based on the level-set model and the contourlet multiresolution analysis. The Hough transform is adapted to yield the initial contours of lumen border and media-adventitia borders.

In [24], Ciompi *et al.* assumed only a few regions can be recognized as media-adventitia, and this region can determine using spatial features of the vessel. Based on that assumptions, they used a polar view to classify the region and detect the border.

Table 1 briefly presents those works that had been described in term of the ability to detect inner and outer border of the IVUS, and technique used. For catheter shape detection, we found most of the works not mentioned about this region except Hamdi *et al.* where they used Hough Transform algorithm to detect the region and used as initial points for IVUS segmentation. In [19], this region is removed and in [25], they set the initial points around the catheter region to segment the lumen. As we mentioned before, there are various techniques used for IVUS segmentation, where the experiment methods also vary and various aspects should be considered [9]. Balocco *et al.* have discussed many aspects of evaluating IVUS segmentation [26].

An example the study that used Snake algorithm to detect lumen and media-adventitia is by Zhu *et al.* [25]. This study used nonlinear filtering and added balloon force to ensure the convergence move to the border smoothly. Zheng *et al.* [27] also proposed Snake algorithm to detect the borders.

3. Methodology

In this research, we start with data collection and pre-processing the images. Next is the step to detect the catheter shape followed by the inner and outer layer detection using deformable model.

3.1. Pre-Processing Image

Preprocessing as an essential step in image processing procedure to remove noise from the image and enhance the quality of image for further process[28], [29]. 30 samples of IVUS image were selected from three (3) patients data that we collected from a repository of Catheterization Lab, Clinical Training Centre (CTC), Universiti Teknologi MARA (Sg.Buloh), Selangor, Malaysia.

In this study, a median filter (3x3), Gaussian filter (3x3) and contrast adjustment techniques were compared. Fig. **1** shows the comparison between those preprocessing techniques. Contrast adjustment preprocessing was selected because it promises better visualization of the image and widely used for medical image processing [30].
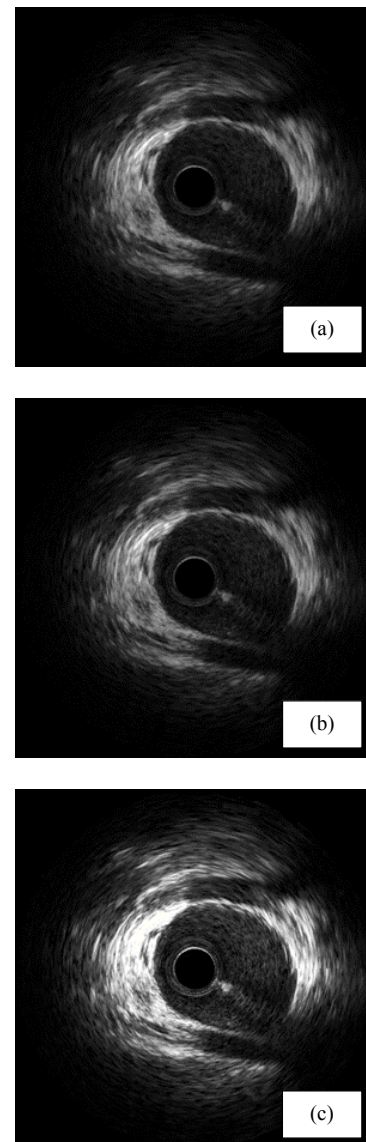

Fig. 1: A Sample of Original IVUS Image after Preprocessing (a) Median filtering (b) Gaussian filtering (c) Contrast Adjustment

Table 1: A list of Previous Works on IVUS Segmentation Process

Ref.	Image Acquisition	Preprocessing &Filtering	(CS)	(L)	(MA)	Technique
[5]	538 images	Applied polar coordinate transformation. Mean Filter.		/	/	Artificial Neural Network with Active Contour Model
[19]	11 Samples Taken from Volcano Website with Reference Size: 512 x 512	Applied polar coordinate transformation. Median filter	Removed	/		The combination of algorithms including Haar wavelet to estimate the lumen boundary
[20]	147 images System: Boston Scientific Size: 512 x 512	Fuzzy contrast enhancement technique		/		Seed selection and random walks algorithm
[3]	System: Volcano IVG3 IVUS Size: 500 x 500	Applied polar coordinate transformation		/	/	Lumen: Fuzzy and threshold approach Media Adventitia: Fast marching technique
[1], [28]	Dataset B [26]			/	/	Otsu thresholding and morphological operation
[10]	50 IVUS images Size: 356 x 356	Applied contourlet transform	/	/	/	Morphological Snake
[21]	2293 IVUS images Size: 256 x 256	Laplacian operator		/	/	Temporal Texture Analysis
[22]	20 MHz intravascular ultrasound (IVUS) image sequences			/	/	Graph-Based Segmentation - Layered Optimal Graph Image Segmentation of Multiple Objects and Surfaces (LOGISMOS)
[23]	Using simulated images and real IVUS images.	Applied contourlet transform		/	/	Level Set Method and contourlet transform
[24]	A dataset with 20MHz/40MHz IVUS system	Applied polar coordinate transformation			/	Classifications based on morphological regions
[25]	20 images (aorta of rabbits) from 40MHz IVUS system. Size: 512 x 512			/	/	Gradient Vector Flow (GVF) Snakes.
[27]	IVUS images	Applied Canny Edge Detection and Circle Hough Transform		/	/	Gradient Vector Flow (GVF) Snakes

(CS): Catheter Shape (L): Lumen (MA): Media-Adventitia

3.2. Catheter Shape Detection

The shape of the IVUS catheter can be seen in the middle of the IVUS image as one complete circle, and the pattern is solid. It is important to detect this shape because the boundary of the shape not only can be used as initial points in the inner layer segmentation process, it is also usable in the trajectory reconstruction for image registration with Angiography modality.

Based on the literature review, only Hamdi et al. detect the region to be used as initialization points for lumen segmentation. The work used a well-known algorithm to detect circular shape which is Hough Transform's algorithm. According to [31], the technique provides a promising result for clear circular structures but complex in the parameter. As an alternative to catheter shape detection using Hough Transform approach, we offer new algorithm to detect the shape. It starts by preprocessing the image to highlight the region and reduce the speckle noise. The next step is to separate the region using threshold technique. To smooth the region, we have normalized the threshold value. After that, the region is labeled, and the center point value of the image is assigned as initial. Then the shape of the catheter is extracted. Lastly, the boundary is plotted on the original image and we store the value, the x- and y-coordinates of the boundary. Fig. **2** shows the sample of IVUS image and the location of catheter shape.
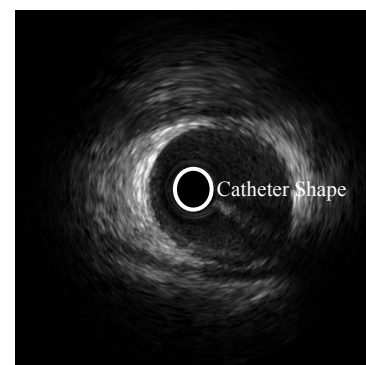
Fig. 2: An Original Image of IVUS with Catheter Shape Location.

3.2.1. Threshold Value Normalization

The threshold is a simple technique to separate the region based on the image intensity specific value before the binary image is created. After preprocessing for 30 images were completed, the threshold value for each sample was determined. The range of pixel intensity value was adjusted using normalization between 0 to 1. The purpose of the adjustment is to highlight the appearance of the shape and to easily detect it in the next phase. The samples were tested with the minimum and maximum value of 0 and 1 respectively. From the observation, the maximum value is divided into two (2) makes it 0.5. and afterward 0.25, 0.05, 0.025 and

0.0125. The last value is selected, as the suitable normalization value that can project the catheter shape region on the IVUS image.

3.2.2. Labeling and extraction

Afterward, the samples go through labeling process. The connected component labeling algorithm has been described in [32]. The algorithm will compute all the connected components in a binary image. The result is a matrix that contains the number of connected regions and the label of each region. So, the center point of the image is initialized as (256,256), according to the height and width of the image as shown in the schematic diagram in Fig. **3**.
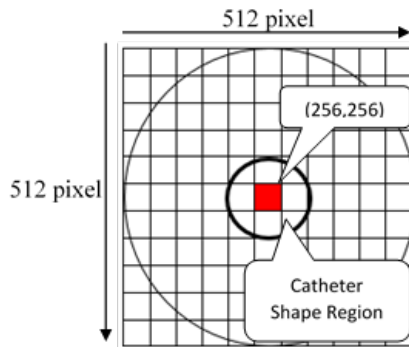
Fig. 3: The Center Point Surrounded by the Catheter Shape Region.

The reason is, the catheter shape region is in the middle of the IVUS image. Extraction of the region was done according to the label of the center point. The rule is if the label is not equal to the center point's label, the label will be changed to zero (0) that means 'black' and if true, the label changed to one (1), white. Fig. **4** shows the pseudo code for the labeling and extraction process. An example of the output shown in Fig. **5**(a).

```
1.BEGIN
2.    Label the binary image;
3.    Initial CenterPoint as (256,256);
4.    Extract the label for CenterPoint;
5.        For each rows and columns
6.            If the label not equal to CenterPoint's label
7.                label equal to 0;
8.            Else
9.                label equal to 1;
10.           End(If)
11.       End(For)
12.END
```

Fig. 4: The Pseudo Code for Extraction and Labelling Process.

3.2.3. Boundary Detection and Plotting

The boundary is a connected set of points that surrounded the interior points. From the result of the detection, the boundary of the catheter shape was traced and plotted to the original image as presented in Fig. **5**(b).
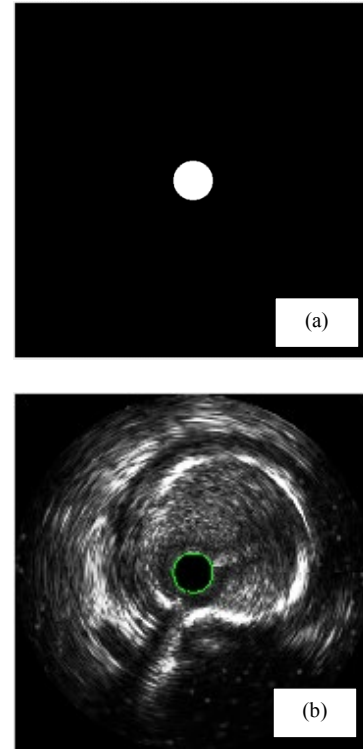
Fig. 5: (a) Catheter Shape Detection after Labeling and Extraction Process. (B): Boundary of Catheter Shape was Plotted on the Original Image.

3.3. Inner and Outer Layer Detection

3.3.1 Deformable Model

Deformable model is a high-level segmentation method where the curves or surfaces move within an image under the influence of internal forces and external forces [33]–[36]. The internal forces defined within the curve or surface to keep the model smooth during deformation, while the external forces computed from the image data as the purpose to move the model toward the boundary[33]–[36]. There are two types of deformable models, parametric and geometric deformable models. Parametric Deformable models explicitly represent the curves and surfaces in their parametric forms during the deformation [36]. For the second type of deformable models, the implicit forms are used to handle the topological changes in an image based on the theory of curve evolution and the level set method [37].

Active contour or snakes are one type of parametric deformable model proposed by [38]. It was started by Snakes algorithm search for minimal energy state expressed as a set of points, (x,y) that defines a function:

$$v(s) = \big(x(s), y(s)\big), s \in [0,1] \tag{1}$$

where s is a member between 0 and 1.

The Snake's energy functions measure the appropriateness of the contour is defined as:

$$E_{snake} \int_0^1 (E_{int}\big(v(s)\big) + E_{ext}(v(s)))ds \tag{2}$$

Where E_{int} in (2) represents the internal energy of the snake and

E_{ext} is external energy. The internal energy of the snake can be represented as:

$$E_{int} = \alpha|v'(s)|^2 + \beta|v''(s)|^2 \tag{3}$$

Where $v'(s)$ and $v''(s)$ are the first and second order derivatives respectively that force the contour to be continuous and to be smooth. The weighting parameters α control the stretch between the points and β control the curvature. The external energy of the snake $E_{ext}(v(s))$ can be defined as an energy that we extract from the image to emphasize the region so that the contour attracts towards the closest boundaries. In this work, Gradient Vector Flow (GVF) introduced by Xu and Prince [35] was used as the external energy. As reported in [34], this technique has an advantage in shaping contour into boundary concavities. Other than that the works in [7], [18] proven that the Snake GVF is the best method for lumen area and border detection.

3.3.2. Lumen Detection

The inner or lumen contour initialization points are required to guide the GVF algorithm to do the segmentation. For the algorithm, the value of parameters α and β are 0.15 and 0.05 respectively. The initialization points move to the expected region and draw a significant line around the expected region. Fig. **6** shows the detected lumen border for the sample of IVUS image.

3.3.3. Media-Adventitia Detection

From the result of the inner layer detection, we set it as the initializations points for outer layer detection. Once again, the deformable model algorithm used in this process and the sample of the detection shows in Fig. **7**.
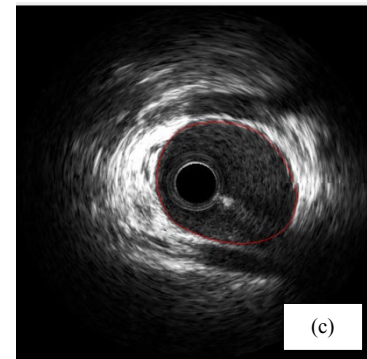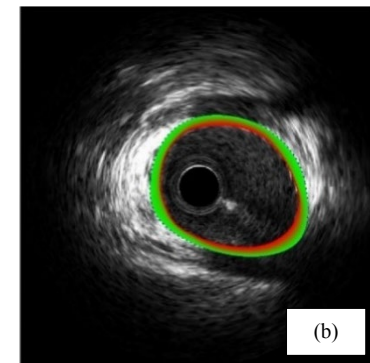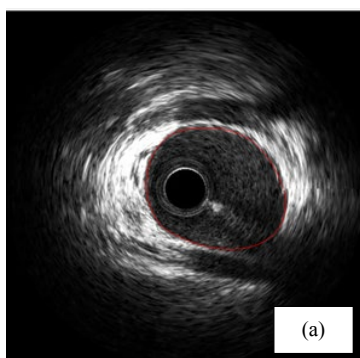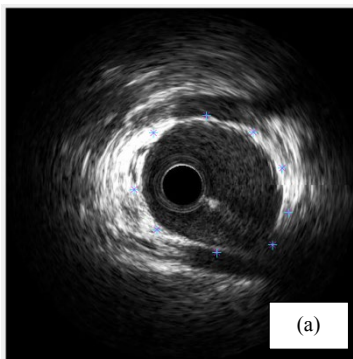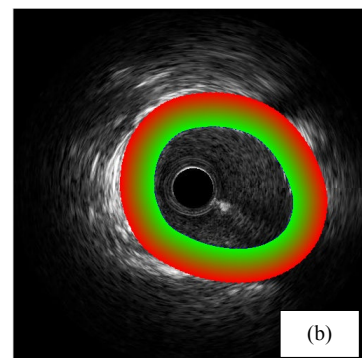

(a)

(a)

(b)

(c)

Fig. 6: Inner Border Detection Process. (a) Initialization points (b) Snake GVF Segmentation (c) Inner Border Detected

4. Results and Discussion

The implementation of the algorithm to detect the catheter shape was performed on 30 IVUS cross-sectional images. The proposed algorithm identified 30 regions of catheter shape on the images. Using the same IVUS images, the proposed algorithm was compared with the Hough Transform algorithm [39], which directly detect the circle shape. This algorithm used by [10] to detect the circle shape in IVUS image as automatic initialization points for their developed segmentation method. As the result, the proposed method successfully detects the catheter shape in all images, but the existing algorithm managed to detect the circle shape on the 28 images, failed to detect the catheter shape in two images. The evaluation results show in Table 2 implies that the proposed algorithm is better than the Hough Transform's method. The proposed algorithm is 100% accurate in detecting the circle shape of the catheter, while the accuracy of the state-of-the-art method was 96.5%.
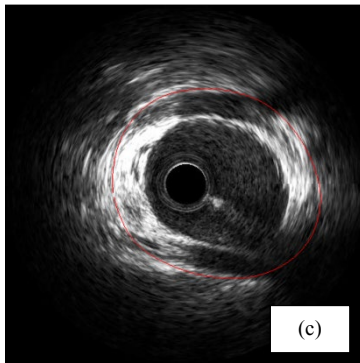

(b)

Fig. 7: Outer Layer Detection Process. (A) Initialization Points (B) Snake GVF Segmentation (C) Outer Border Detected.

Table 2: Comparison between the Proposed Method and the Hough Transform's Method

Performance Measurement	PROPOSED METHOD	Hough Transform's Method
Precision	100	100
Recall	100	93
Accuracy	100	96.5

In the first stage of this proposed method, we used contrast adjustment as the technique to enhance the IVUS image. The contrast adjustment technique was selected is due to the advantage of it in keeping the details of the image. This technique always used in medical image preprocessing step because it could maintain the quality of the image [30]. We proposed to use 0.0125 as a value to normalize the image intensity after many values were tested accordingly. Using this normalized threshold value make the catheter shape region in the IVUS image being spotted clearly and the noise around the region was decreased. Labeling and extraction process is still needed because we want to trace the boundary of the catheter shape. The value that we store could be used in lumen segmentation process and usable in trajectory reconstruction.

For inner and outer layer detection, two cardiologists from the Clinical Training Centre (CTC), University Technology Mara (Sg.Buloh) segmented the same data images manually to evaluate the results of the experiment. These data were used as manual reference segmentations drawn by experts normally approximate ground truth and the experts were blinded to the other cardiologist's segmentation and to the results of the proposed method. The sample of the annotations from the gold standard and the proposed method's results for inner and outer borders as shown in Fig. **8**, where the blue line represents one of the gold standard segmentation and the red line is our detection results.
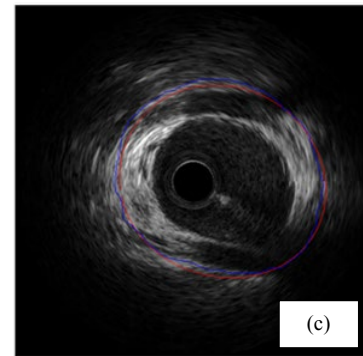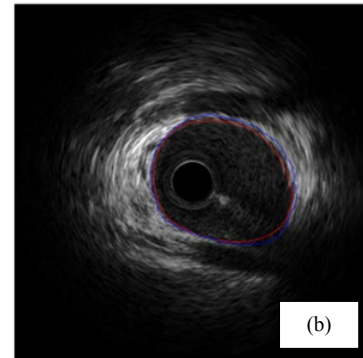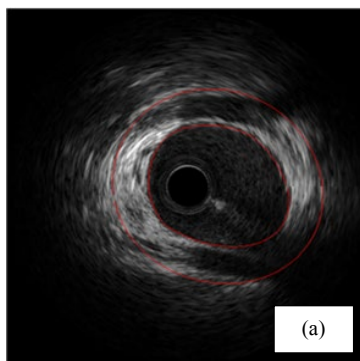

Fig. 8: (a) Inner and Outer Layers have been Detected (B) Inner Border Detection of the Proposed Method Compared to the Gold Standard (C) Outer Border Detection of the Proposed Method Compared to the Gold Standard.

The distribution of the result for lumen and media-adventitia segmentation between experiment and the gold standard shown in Fig. **9** and Fig. **10** respectively. As can be seen, the area of lumen detected by proposed method approaches the value segmented by the reference 2. However, in the media-adventitia segmentation, the values obtained by the proposed method closer to the value obtained by the reference 1.

Percentage Area of Difference (PAD) [1], [26] is used to evaluate the difference of the lumen area for the proposed method and the gold standard segmentation. PAD is computed as:

$$PAD = \frac{|A_{auto} - A_{man}|}{A_{man}} \qquad (4)$$

The value should be zero if the segmentation is perfect [1]. The results of this work can be seen in Table 3.

From the table, the PAD for lumen segmentation between the experiment and the first ground truth is 0.27 and for the media-adventitia segmentation is 0.10. Comparison with second ground truth, the lumen segmentation is 0.07 and media-adventitia is 0.31. Even our segmentation result is highly encouraging, yet we also determined the change between both references, 0.16 for lumen and 0.28 for outer layer segmentation. The variability of the results implies that the existing of the inter observation in the process of manual segmentation. To ensure the finding is acceptable in the clinical practice, it is suggested to have odd numbers of reference and the variability of the finding should be reviewed by the expert.

Table 3: The Average Of PAD Value for Lumen and Media-Adventitia Segmentation Between the Proposed Method and the Gold Standards.

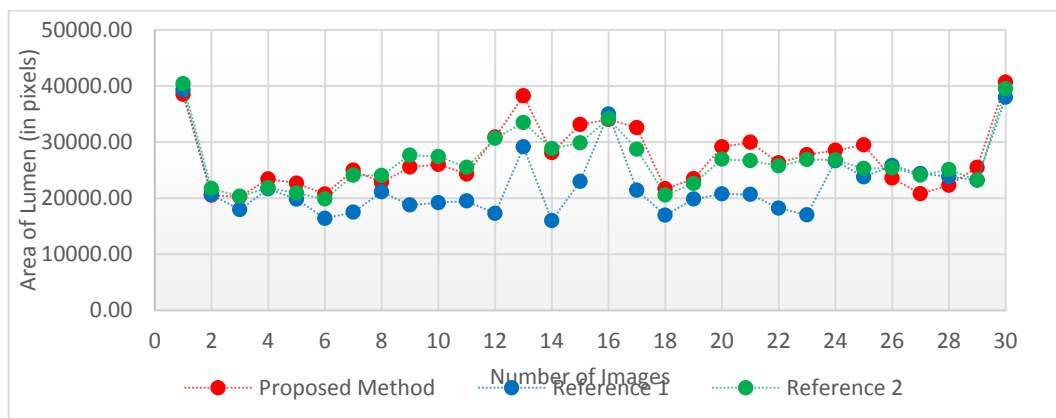| PAD	Lumen	Media-Adventitia
Experiment : Reference 1	0.27	0.10
Experiment : Reference 2	0.07	0.31
Reference 1 : Reference 2	0.16	0.28

Fig. 9: Area of Lumen for 30 IVUS Images Between the Proposed Method Compared to the Gold Standard Segmentation.
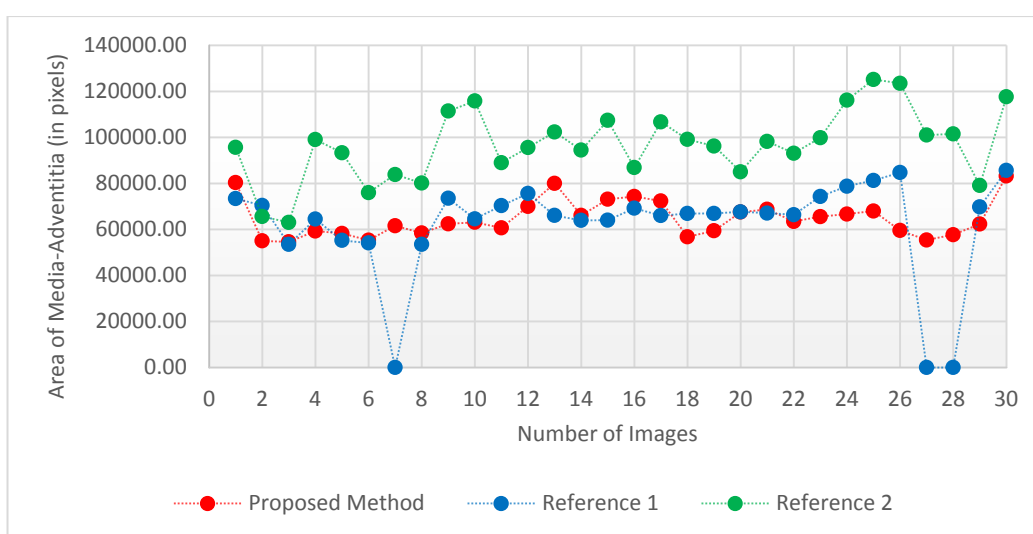

Fig. 10: Area of Media-Adventitia for 30 IVUS Images between the Proposed Method Compared to the Gold Standard Segmentation.

5. Conclusion

In conclusion, this paper describes the complete process of IVUS segmentation. A new algorithm to detect and segment the catheter shape is introduced. From the experiments, the algorithm has successfully segmented the shape with 100% accurate. The output from this segmentation could be used as correspondence points to merge IVUS and Angiography modality. After that, we used the parametric deformable model to detect an inner and outer layer of the IVUS. The combination of parametric deformable algorithm and the gradient vector flow energy allow better performance in the segmentation. The result of inner detection border could be used as initial points to the media-adventitia detection.

Acknowledgment

References

[1] H. Sofian, J. C. M. Than, N. Mohd Noor, and H. Dao, "Segmentation and detection of media adventitia coronary artery boundary in medical imaging intravascular ultrasound using Otsu thresholding," in *BioSignal Analysis, Processing and Systems (ICBAPS), 2015 International Conference on*, 2015, pp. 72–76.

[2] F. S. Zakeri, S. K. Setarehdan, and S. Norouzi, "Automatic media-adventitia IVUS image segmentation based on sparse representation framework and dynamic directional active contour model," *Comput. Biol. Med.*, no. March, pp. 1–12, 2017.

[3] J. Yan and Y. Cui, "A novel approach for segmentation of intravascular ultrasound images," in *Bioelectronics and Bioinformatics (ISBB), 2015 International Symposium on*, 2015, pp. 51–54.

[4] M. B. Tayel, M. A. Massoud, and Y. Farouk, "A modified segmentation method for determination of IV vessel boundaries," *Alexandria Eng. J.*, vol. 56, no. 4, pp. 449–457, 2017.

[5] S. Su, Z. Gao, H. Zhang, Q. Lin, W. K. Hau, and S. Li, "Detection of lumen and media-adventitia borders in ivus images using sparse auto-encoder neural network," in *2017 IEEE 14th International Symposium on Biomedical Imaging (ISBI 2017)*, 2017, pp. 1120–1124.

[6] C. H. Chen and A. G. Gangidi, "Automatic Segmentation of Intravascular Ultrasound Images based on Temporal Texture Analysis," *Comput. Cardiol. (2010).*, vol. 41, pp. 957–960, 2014.

[7] R. Sanz-Requena, D. Moratal, D. R. García-Sánchez, V. Bodí, J. J. Rieta, and J. M. Sanchis, "Automatic segmentation and 3D

reconstruction of intravascular ultrasound images for a fast preliminar evaluation of vessel pathologies," *Comput. Med. Imaging Graph.*, vol. 31, pp. 71–80, 2007.

[8] D. D. Patil and S. G. Deore, "Medical Image Segmentation : A Review," *Int. J. Comput. Sci. Mob. Comput.*, vol. 2, no. 1, pp. 22–27, 2013.

[9] A. Katouzian, E. D. Angelini, S. G. Carlier, J. S. Suri, N. Navab, and A. F. Laine, "A state-of-the-art review on segmentation algorithms in intravascular ultrasound (IVUS) images," *IEEE Trans. Inf. Technol. Biomed.*, vol. 16, no. 5, pp. 823–834, 2012.

[10] M. A. Hamdi, K. S. Ettabaa, M. L. Harabi, and L. Alvarez, "Real time IVUS segmentation and plaque characterization by combining morphological snakes and contourlet transform," in *Recent Advances in Biomedical & Chemical Engineering and Materials Science*, 2014, pp. 160–166.

[11] M. Papadogiorgaki, V. Mezaris, Y. S. Chatzizisis, G. D. Giannoglou, and I. Kompatsiaris, "Image Analysis Techniques for Automated IVUS Contour Detection," *Ultrasound Med. Biol.*, vol. 34, no. 9, pp. 1482–1498, 2008.

[12] A. Taki *et al.*, "Automatic segmentation of calcified plaques and vessel borders in IVUS images," *Int. J. Comput. Assist. Radiol. Surg.*, vol. 3, pp. 347–354, 2008.

[13] Q. Zhang, Y. Wang, W. Wang, M. Jianying, J. Qian, and J. Ge, "Contour extraction from IVUS images based on GVF snakes and wavelet transform," in *2007 IEEE/ICME International Conference on Complex Medical Engineering*, 2007, pp. 536–541.

[14] G. D. Giannoglou *et al.*, "A novel active contour model for fully automated segmentation of intravascular ultrasound images: In vivo validation in human coronary arteries," *Comput. Biol. Med.*, vol. 37, no. 9, pp. 1292–1302, 2007.

[15] M.-H. R. Cardinal, J. Meunier, G. Soulez, R. L. Maurice, E. Therasse, and G. Cloutier, "Intravascular ultrasound image segmentation: a three-dimensional fast-marching method based on gray level distributions.," *IEEE Trans. Med. Imaging*, vol. 25, no. 5, pp. 590–601, 2006.

[16] E. Brunenberg, O. Pujol, B. ter Haar Romeny, and P. Radeva, "Automatic IVUS segmentation of atherosclerotic plaque with stop & go snake.," *Med. Image Comput. Comput. Assist. Interv.*, vol. 9, no. Pt 2, pp. 9–16, 2006.

[17] G. Unal, S. Bucher, S. Carlier, G. Slabaugh, T. Fang, and K. Tanaka, "Shape-driven Segmentation of Intravascular Ultrasound Images," in *Proc MICCAI Workshop in Computer Vision for Intravascular and Intracardiac Imaging*, 2006, pp. 50–57.

[18] M. E. Plissiti, D. I. Fotiadis, L. K. Michalis, and G. E. Bozios, "An Automated Method for Lumen and Media–Adventitia Border Detection in a Sequence of IVUS Frames," *IEEE Trans. Inf. Technol. Biomed.*, vol. 8, no. 2, pp. 131–141, Jun. 2004.

[19] M. Eslamizadeh, G. Attarodi, N. J. Dabanloo, and J. F. Sedehi, "The Segmentation of Lumen Boundaries at Intravascular Ultrasound Images Using Fuzzy Approach," in *2017 Computing in Cardiology (CinC)*, 2017, vol. 44, pp. 1–4.

[20] Debarghya China, M. K. Nag, K. M. Mandana, A. K. Sadhu, P. Mitra, and C. Chakraborty, "Automated in vivo delineation of lumen wall using intravascular ultrasound imaging," in *2016 38th Annual International Conference of the IEEE Engineering in Medicine and Biology Society (EMBC)*, 2016, pp. 4125–4128.

[21] C. H. Chen and A. G. Gangidi, "Automatic Segmentation of Intravascular Ultrasound Images based on Temporal Texture Analysis," in *Computing in Cardiology*, 2014, pp. 957–960.

[22] S. Sun, M. Sonka, and R. R. Beichel, "Graph-based ivus segmentation with efficient computer-aided refinement," *IEEE Trans Med Imaging*, vol. 32, no. 8, pp. 997–1003, 2013.

[23] H. Lazrag and M. S. Naceur, "Combination of the level-set methods with the contourlet transform for the segmentation of the IVUS images," *Int. J. Biomed. Imaging*, vol. 2012, 2012.

[24] F. Ciompi, O. Pujol, C. Gatta, X. Carrillo, J. Mauri, and P. Radeva, "A Holistic approach for the detection of media-adventitia border in IVUS," *Lect. Notes Comput. Sci. (including Subser. Lect. Notes Artif. Intell. Lect. Notes Bioinformatics)*, vol. 6893 LNCS, no. PART 3, pp. 411–419, 2011.

[25] X. Zhu, P. Zhang, J. Shao, Y. Cheng, Y. Zhang, and J. Bai, "A snake-based method for segmentation of intravascular ultrasound images and its in vivo validation," *Ultrasonics*, vol. 51, no. 2, pp. 181–189, 2011.

[26] S. Balocco *et al.*, "Standardized evaluation methodology and reference database for evaluating IVUS image segmentation,"

[27] *Comput. Med. Imaging Graph.*, vol. 38, no. 2, pp. 70–90, 2014.

[27] M. Zheng, W. Yubin, W. Yousheng, S. Xiaodi, and W. Yali, "Detection of the lumen and media-adventitia borders in IVUS imaging," in *International Conference on Signal Processing Proceedings, ICSP*, 2008, vol. 1, no. 1, pp. 1059–1062.

[28] D. A. Kumar, "A new Method on Brain MRI Image Preprocessing for Tumor Detection," *Int. J. Sci. Res. Sci. Eng. Technol.*, vol. 1, no. 1, pp. 40–44, 2015.

[29] N. Shameena and R. Jabbar, "A Study of Preprocessing and Segmentation Techniques on Cardiac Medical Images," *Int. J. Eng. Res. Technol.*, vol. 3, no. 4, pp. 336–341, 2014.

[30] V. Rajamani, S. Jaiganesh, and P. Babu, "A review of various global contrast enhancement techniques for still images using histogram modification framework," *Int. J. Eng. Trends Technol.*, vol. 4, no. 4, pp. 1045–1048, 2013.

[31] A. Mölder, S. Czanner, N. Costen, and G. Hartshorne, "Automatic detection of embryo location in medical imaging using trigonometric rotation for noise reduction," in *Proceedings - International Conference on Pattern Recognition*, 2014, pp. 3239–3244.

[32] R. C. Gonzalez, R. E. Woods, and S. L. Eddins, *Digital Image Processing Using MATLAB*, Second., vol. Second Ed. Gatesmark,LLC,USA: Pearson Education,Inc, 2011.

[33] C. Xu, "Deformable Models with Application to Human Cerebral Cortex Reconstruction from Magnetic Resonance Images," 1999.

[34] C. Xu and J. L. Prince, "Snakes, shapes, and gradient vector flow," *IEEE Trans. Image Process.*, vol. 7, no. 3, pp. 359–369, 1998.

[35] Xu, Chenyang and J. L. Prince, "Gradient vector flow: a new external force for snakes," *Proc. IEEE Comput. Soc. Conf. Comput. Vis. Pattern Recognit.*, vol. 2, no. 1, pp. 66–71, 1997.

[36] C. Xu, D. Pham, and J. Prince, "Chapter 3: Image segmentation using deformable models," in *Handbook of Medical Imaging*, 2000, pp. 129–174.

[37] A. Farag, Ed., *Deformable Models - Theory and Biomaterial Applications*, 1st ed. Springer-Verlag New York, 2007.

[38] M. Kass, A. Witkin, and D. Terzopoulos, "Active contour models," *Int. J. Comput. Vis.*, vol. 1, no. 4, pp. 133–144, 1987.